
DIODE PUMPED FREQUENCY DOUBLED YAG LASER FOR THE TREATMENT OF GLAUCOMA

Rafael A. Sierra

**Fiberoptic Fabrications, Inc.
515 Shaker Road
East Longmeadow, MA 01028**

August 1996

Final Report

19970113 119

APPROVED FOR PUBLIC RELEASE; DISTRIBUTION IS UNLIMITED.



**PHILLIPS LABORATORY
Lasers and Imaging Directorate
AIR FORCE MATERIEL COMMAND
KIRTLAND AIR FORCE BASE, NM 87117-5776**

Using Government drawings, specifications, or other data included in this document for any purpose other than Government procurement does not in any way obligate the U.S. Government. The fact that the Government formulated or supplied the drawings, specifications, or other data, does not license the holder or any other person or corporation; or convey any rights or permission to manufacture, use, or sell any patented invention that may relate to them.

This report has been reviewed by the Public Affairs Office and is releasable to the National Technical Information Service (NTIS). At NTIS, it will be available to the general public, including foreign nationals.

If you change your address, wish to be removed from this mailing list, or your organization no longer employs the addressee, please notify PL/LIDA, 3550 Aberdeen Ave SE, Kirtland AFB, NM 87117-5776.

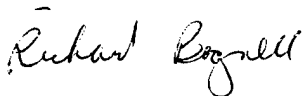
Do not return copies of this report unless contractual obligations or notice on a specific document requires its return.

This report has been approved for publication.



PETER S. DURKIN
Project Manager

FOR THE COMMANDER



RICHARD BAGNELL
Chief, Semiconductor Laser Branch



ROBERT A. DURYEA, Col, USAF
Director, Lasers and Imaging Directorate

DRAFT SF 298

1. Report Date (dd-mm-yy) August 1996		2. Report Type Final Report		3. Dates covered (from... to) 12 Dec 95 - 12 Jun 96	
4. Title & subtitle DIODE PUMPED FREQUENCY DOUBLED YAG LASER FOR THE TREATMENT OF GLAUCOMA				5a. Contract or Grant # F29601-95-C-0198	
				5b. Program Element # 65502F	
6. Author(s) Rafael A. Sierra				5c. Project # STTR	
				5d. Task # C0	
				5e. Work Unit # AD	
7. Performing Organization Name & Address Fiberoptic Fabrications Inc. 515 Shaker Road East Longmeadow, MA 01028				8. Performing Organization Report #	
9. Sponsoring/Monitoring Agency Name & Address Phillips Laboratory 3550 Aberdeen Avenue, SE Kirtland AFB, NM 87117-5776				10. Monitor Acronym LIDA	
				11. Monitor Report # PL-TR-96-1178	
12. Distribution/Availability Statement Approved for Public Release; Distribution is Unlimited					
13. Supplementary Notes					
14. Abstract The Phase I STTR technical effort demonstrated the safety and efficiency of a continuous wave (cw) diode pumped frequency doubled YAG laser for the treatment of glaucoma. In-vitro and in-vivo experiments were conducted to establish safety and to identify the procedures best suited for this laser. The laser was fabricated according to a design developed at the Air Force Phillips Laboratory. The most significant result of the work was the verification of the assumption that the cw diode pumped frequency doubled YAG laser effects a tissue response nearly identical to that observed with an argon ion laser at identical power, spot size, and pulse duration. In-vitro exposure of ocular tissue with both lasers showed an acute response consistent with a thermal process. The use of the frequency doubled YAG laser to treat retinal tissue and for laser suturelysis was also investigated. These additional tests extend the potential of the laser to encompass all ophthalmic applications currently performed with the argon ion laser.					
15. Subject Terms Solid-state lasers, frequency doubling, diode pumped, glaucoma					
Security Classification of			19. Limitation of Abstract Unlimited	20. # of Pages 40	21. Responsible Person (Name and Telephone #) Maj Peter S. Durkin 505-846-5913
16. Report Unclassified	17. Abstract Unclassified	18. This Page Unclassified			

CONTENTS

	PAGE
I. Introduction	1
II. Description of Phase I Results	3
II.1 Laser Development	3
II.2 In-vitro and In-vivo Tests	15
II.3 Investigation of Rectangular Core Fiber	22
III. Discussion	25
IV. Phase II Objectives	26
V. Conclusions and Recommendations	30
VI. Literature Cited	32

FIGURES

<u>FIGURE</u>	<u>PAGE</u>
1. Folded resonator design.	4
2. nth round trip.	6
3. Predicted output using single waist resonator.	11
4. Beam radius as a function of position using a single waist resonator.	12
5. Beam radius as a function of position using a symmetric waist resonator.	12
6. Predicted output using the symmetrical waist resonator.	13
7. Laser diode array output.	13
8. Temperature dependence of diode array output.	14
9. YAG laser output.	15
10. Scanning electron micrograph showing planar view of iris.	18
11. Light micrograph showing cross section view of two iridectomies.	19
12. Scanning electron micrograph showing an iridectomy produced by the argon laser.	20
13. Scanning electron micrograph showing an iridectomy produced by the DPFdNd:YAG laser.	21
14. Cylindrical lens on fiber tip approximating a hyperbolic shape.	24
15. Measured profile of cylindrical lens on fiber tip.	25

I. Introduction

Glaucoma is a potentially blinding disease due to progressive optic nerve damage. This optic nerve damage is usually associated with elevated intraocular pressure above 21 mmHg, although glaucomatous optic nerve damage may occur even in the absence of an elevated intraocular pressure. Typically, patients with glaucoma initially lose peripheral vision then gradually lose visual acuity.

Glaucoma is among the leading causes of blindness in the United States and other industrialized countries.^{1,2} At least 2 million Americans have the disease, and nearly 80,000 Americans are blind from glaucoma. Certain subsets of the US population have an even higher prevalence of glaucoma than the general population. Recently, it has become clear that glaucoma is the leading cause of blindness among African Americans.³⁻⁹ In the Baltimore eye survey, African Americans had a prevalence of open-angle glaucoma four to five times higher than whites, with a prevalence of glaucoma as high as 11% in those 80 years or older.¹⁰

Laser therapy has been useful for non-invasive treatment of angle-closure glaucoma¹¹ and open-angle glaucoma.^{12,13} Laser iridectomy is an effective procedure for the treatment of angle closure glaucoma. Similarly, laser trabeculoplasty is effective, with 50% success rate after 5 years.¹⁴ Moreover, laser sclerostomy shows promise as a definitive procedure for the treatment of intractable glaucoma.¹⁵

Argon ion lasers are commonly used in the treatment of glaucoma as well as other ophthalmic diseases. For example, retinal diseases such as macular degeneration that are caused by leakage of blood from vessels near the optic nerve are treated by photocoagulation. Glaucoma is routinely treated by iridectomy and trabeculoplasty using argon ion lasers. Other procedures such as vitrectomy commonly involve the use of argon ion lasers. The argon ion laser is, in many cases, the standard of care with a long and well established clinical history.

The typical argon ion laser used in many of the procedures above has continuous wave (cw) output power in the range of 0.5 to 1.5 w. The laser wavelength is 514 nm. Commonly the lasers are relatively large and often require 208 volt 3 ϕ power and water cooling. Although manufacturers have made impressive improvements in the reliability of the lasers, there remains a relatively high maintenance tube that must be replaced at high cost to the user.

Recently, the development of high power diode pumped lasers makes possible an all solid state replacement to the argon ion laser. Specifically a number of groups have now

reported frequency doubled, diode pumped, Nd:YAG lasers with output power in excess of 1 w at 532 nm. Such lasers can operate from common 110V AC sources, require only air cooling, and are potentially maintenance free. Their clinical performance may be reasonably expected to be largely similar to that of the argon ion laser and this laser should be relatively well accepted by the ophthalmic community.

Recently, researchers at the Air Force Laboratory (PL) have demonstrated a cw 2.0 w output power, frequency doubled Nd:YAG laser pumped by diode laser sources.²⁸ This laser is a strong candidate to replace a number of lasers, particularly ion lasers, in ophthalmology. Fiberoptic Fabrications Inc. (FFI), in collaboration with the Massachusetts Eye and Ear Infirmary (MEEI), has investigated the use of the diode pumped cw frequency doubled YAG laser for noninvasive therapy of glaucoma. The work has demonstrated the safety of the cw frequency doubled YAG laser for the treatment of glaucoma. In addition the development of the PL design into a commercially viable laser source has been undertaken. The resulting product will be marketed throughout the CeramOptec group of companies. This international group of companies already markets lasers and laser delivery systems developed and manufactured by Fiberoptics Fabrications Inc.

The diode pumped frequency doubled YAG laser can be expected to produce very similar tissue response as that to the argon ion laser. The mode of operation of the two lasers is the same (cw) and the available power similar. The key difference among the two lasers is the output wavelength. The ion laser operates at 514 nm while the frequency doubled YAG operates at 532 nm. This small difference in wavelength results in greater depth of penetration of the frequency doubled YAG laser into the tissue and stronger absorption by oxy-hemoglobin. This small but significant difference may suggest a modified treatment protocol. Investigation of the safety of the cw frequency doubled YAG laser was the key objective of the Phase I effort. The work was carried out in collaboration with the MEEI.

Based on the discussion above, the key objectives for the Phase I effort were established as follows:

1. Assemble a laser system based on the PL design for use in studies assessing the safety of the frequency doubled Nd:YAG laser. Modify a slit lamp to permit delivery of the laser output in conjunction with a gonioscopic lens.
2. Evaluate the use of the frequency doubled YAG laser for the noninvasive therapy of glaucoma. Compare the

response of ocular tissue to this laser with the response obtained using an argon ion laser at identical parameters. In-vitro procedures to be tested included peripheral iridectomy, laser trabeculoplasty and laser sclerostomy. These procedures will then be performed in experimental animals in vivo to assess the safety of the laser.

3. Investigate the use of proprietary high brightness diode laser coupling optical fibers to improve the PL design. The use of high brightness diode laser coupling optical fibers will permit operation of the PL laser at higher output power from a reduced component count.

The work performed to meet these objectives is now presented.

II. Detailed Description of Phase I Results

II.1 Objective 1) Laser Development.

The first objective outlined above was to analyze the PL laser design and to assemble a laser of that design for use in the studies at the collaborators's site. Both computer modeling and experimental studies were carried out resulting in a packaged prototype laser used at the MEEI. The modeling and experimental results follow.

Laser Design

There are a number of factors to be considered while addressing the design of this laser. First, since this laser will operate in continuous wave mode (cw) frequency doubling will need to be carried out intracavity where power density can be high enough to obtain second harmonic generation. Since beam quality and efficiency are key elements, pumping of the lasers must be in the end pumped configuration. In end pumped lasers, the pumped volume can be made to overlap the mode volume of lowest (TEM₀₀) mode of the resonator thus achieving both high efficiency and good beam quality. Not surprising, both lasers reported in the literature and considered as potential candidates were end pumped lasers.

There were two designs that have recently been described in the literature that were considered. One design by D. C. Hanna of South Hampton University uses a ring resonator and a 20 w diode pump. The ring design avoids hole burning in the gain medium and results in single frequency operation. This design does suffer somewhat since

the gain medium is single passed resulting in higher lasing threshold. In addition, the laser requires a Faraday rotator to insure unidirectional operation, a costly component.

A simpler design was described by Durkin and Post of the PL. Their design uses a folded Z as shown below. The design has several features

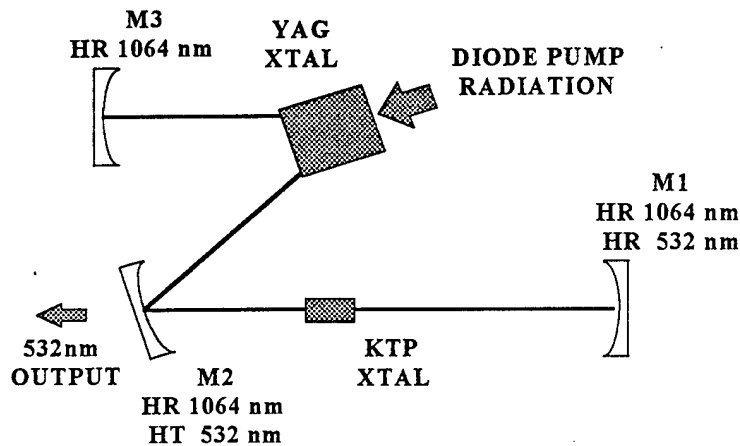


Figure 1
Folded Resonator Design

that can reduce the cost of the laser system. First, by locating the YAG crystal at the apex of one of the folds in the cavity, the crystal is traversed four times each round trip of the radiation. This permits the use of a smaller (lower cost) crystal. The KTP crystal is double passed, again allowing the use of a shorter crystal, and the system needs no costly Faraday rotator. If the angle ϕ is chosen carefully, it can be made to match the numerical aperture of the fiber that delivers the pump radiation, making the coupling optics trivial (actually, they simply disappear). Thus the system is potentially very inexpensive.

Having chosen this design, the selection of actual components is straight forward. First, in order to achieve reasonable doubling efficiency, a tight beam waist is desired at the KTP crystal. Currently, about 16 watts can be delivered to the YAG crystal by means of a single 600um fiber 0.2NA. The maximum power density at the crystal without the use of coupling optics is given by

$$P_{\max} = \frac{16 \text{ watts}}{A_f} = 5.6 \times 10^3 \text{ watts/cm}^2$$

1)

which will be shown to be far above the needed power density. The angle ϕ in Figure 1 is established by the fiber NA to be on the order of 20° .

The process of selecting components according to the criteria described has been divided into three parts. One part is guided by modeling of the intracavity doubling problem and serves to select the KTP crystal and the beam geometry at the YAG and KTP crystals. Next, a resonator is designed that achieves these values. Finally coupling of the laser diodes to the resonator is considered with an eye on reducing system complexity and avoiding existing patents.

Laser Modeling

A simple model of the laser can be developed and used to estimate the performance that can be achieved. Let the power of the radiation circulating inside the laser resonator at 1064nm be given by p . The green power (P_{gr}) generated at the KTP crystal in two passes is given by

$$P_{gr} = 2\eta p^2 \frac{1}{A_k}$$

where η is the doubling efficiency of the crystal, and A_k the beam area at the crystal. Note that for a fixed power p the generated green power increases with decreasing beam area at the KTP crystal. η can be calculated from the crystal non linear parameters and will be given later.

For a cw laser, at steady state, the input pump power must be exactly balanced by the sum of the radiated power, the parasitic losses, and the useful power coupled out of the laser. For the specific case of a laser of the configuration given in Figure 1 one can write a balance equation as follows. First, imagine the laser as an unfolded, repeated sequence of round trip passes. In that case, the n^{th} round trip is as shown below in Figure 2

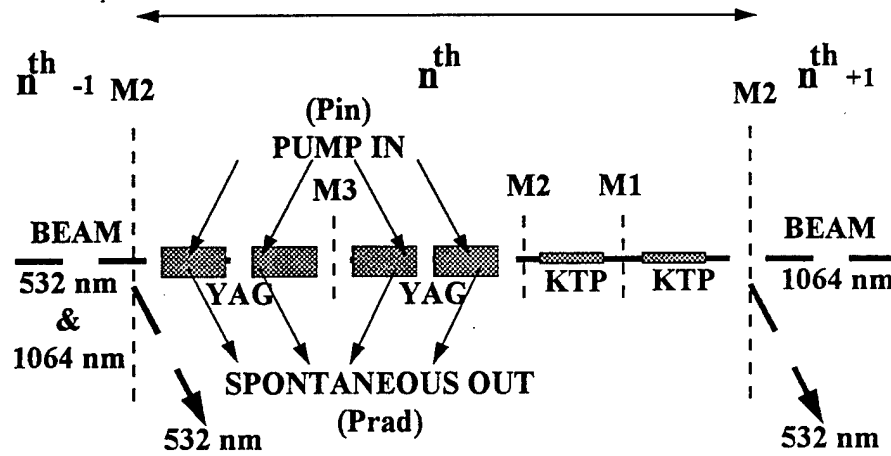


Figure 2
nth Round Trip

From the figure above, we have for a round trip the balance equation

$$4P_{in} = 4P_{rad} + (P_{loss} + P_{out}) \quad (3)$$

The output coupled power P_{out} is given by the sum of equation 2 plus the $1.06\mu\text{m}$ radiation coupled out of the resonator. That is

$$P_{out} = 2\eta \frac{p^2}{A_k} + \frac{(1-r)p}{1+r} \quad (4)$$

Here r is the output coupler reflectivity at $1.06\mu\text{m}$. The parasitic loss for one round trip is, again from the figure, 4 passes through the YAG crystal and two resonator passes, that is

$$P_{loss} = (4\alpha_{YAG} + 2\alpha_r)P \quad (5)$$

Equation 3) can be solved for the radiated power, P_{rad}

$$P_{rad} = P_{in} - 1/4(P_{loss} + P_{out}) \quad 6)$$

P_{in} , the input power at the crystal is given by

$$P_{in} = \eta_a \eta_q \eta_d P_p \quad 7)$$

Here η_a is the fraction of the incident power P_p that is absorbed by the YAG crystal. η_q is the quantum efficiency and η_d the quantum defect between the pump photons (@ 808nm) and laser photons (@ 1064nm). Experience has shown $\eta_q \sim 0.95$. Then, for the case where 85% of the incident power is absorbed one has

$$\eta_a \eta_q \eta_d \sim 0.61 \quad 8)$$

The incident power P_p is just the diode laser pump power which in our case can be up to 16 watts.

Combining equations 4, 5, 6, and 7, the power radiated by the YAG crystal is simply

$$P_{rad} = \eta_a \eta_q \eta_d - \left(\frac{\eta_p}{2A_k} + \alpha_{YAG} + \frac{\alpha_r}{2} \right) p \quad 9)$$

For simplicity we have taken the case where the resonator reflectivity is 100% at 1.06um. At threshold, the circulating power p is essentially zero, and one finds

$$P_{rad} = \eta_a \eta_q \eta_d p_{th} \quad 10)$$

The radiated power can also be calculated from the number of excited Nd^{3+} atoms in the upper laser level (n)

$$P_{rad} = \frac{nh\nu}{\tau} \quad 11)$$

Where $h\nu$ is the photon energy, and τ the radiative lifetime of the upper laser level. Equation 11) can be multiplied and divided by the product $\sigma_e V$ where σ_e is the estimated emission crosssection and V the excited volume to obtain

$$P_{rad} = \frac{nh\nu\sigma_e V}{\tau\sigma_e V} = \frac{nh\nu\sigma_e l A_y}{\tau\sigma_e V} \quad 12)$$

Here l is the YAG crystal length and A_y the beam diameter at the YAG crystal. The quantity

$$\frac{n}{v} \sigma_e l = g_{olT} \quad 13)$$

is the gain at threshold. Similarly the quantity

$$\frac{h\nu}{\tau \sigma_e} = I_{sat} \quad 14)$$

is the saturation intensity. Then using 12, 13, and 14 one can write

$$P_{rad} = g_{olT} I_{sat} A_y \quad 15)$$

Using equation 15, equation 9 becomes

$$g_{olT} I_{sat} A_y = \eta_a \eta_g \eta_d P_p - \left(\frac{\eta_p}{2A_k} + \alpha_{YAG} + \frac{\alpha_r}{2} \right) P \quad 16)$$

which can also be expressed

$$g_{olT} = \frac{\eta_a \eta_g \eta_d I_p}{I_{sat}} - \left(\frac{\eta I_k}{2} + \alpha_{YAG} + \frac{\alpha_r}{2} \right) \frac{I_{YAG}}{I_{sat}} \quad 17)$$

Here I_p is the intensity of the pump diode laser at the YAG crystal, I_k the beam intensity at the KTP crystal, and I_{yag} the beam intensity at the YAG crystal.

For a laser at steady state, the saturated gain is equal to the threshold gain, this is

$$g_{olT} = \frac{g_{ol}}{1.0 + I/I_{sat}} \quad 18)$$

Then, using 17) and noting

$$g_{ol} = \frac{\eta_a \eta_g \eta_d I_p}{I_{sat}} \quad 19)$$

one can write

$$\frac{\eta_a \eta_g \eta_d I_p}{I_{sat}} - \left(\frac{\eta I_k}{2} + \alpha_{YAG} + \frac{\alpha_r}{2} \right) \frac{I_{YAG}}{I_{sat}} = \frac{\eta_a \eta_g \eta_d I_p}{1.0 + I_{yag}/I_{sat}} \quad 20)$$

Next, the reduced intensity I_R is defined

$$I_R = I_{YAG}/I_{SAT} \quad 21)$$

Then 20 may be expressed

$$\frac{\eta_a \eta_g \eta_d I_p}{I_{sat}} - \frac{(\eta I_k + \alpha_{YAG} + \frac{\alpha_r}{2}) I_R}{2} = \frac{\eta_a \eta_g \eta_d I_p}{1.0 + I_R} \quad 22)$$

Equation 22 is conveniently solved numerically on a computer. The only unknown quantities are (assuming the crystal and resonator losses are known) the beam areas at the YAG crystal and the KTP crystal, and the reduced intensity I_R . The beam areas are established by the choice of mirrors in the resonator, and can be varied arbitrarily. In the next section, resonator design will be addressed. Here, A_y and A_k will be varied arbitrarily until the desired green output is achieved. In the next section, mirrors and dimensions will be adjusted to obtain A_y and A_k as established here.

Resonator Design

The basic resonator geometry was selected as shown in Figure 1. It remains however to select the radii of curvature of the mirrors, the YAG crystal, and the spacing between components. These are selected to meet the requirements established in the previous section. In addition, one looks for designs that have strong rejection to high order modes. For simplicity, the design is carried out using Gaussian beam propagation. This is really not a limitation since any other "real" beam can be described by a similar analysis using the scaling formalism described by Siegman and Townsend.

To analyze the resonator described in Figure 1, a computer program was written that uses ABCD matrices to propagate a beam through the various optical elements. The spot size and radius of curvature of the beam are calculated at each point along the resonator path. An eigenmode mode of the resonator is characterized by a beam that retraces itself both in spot size and radius of curvature at each point along the beam path. Mirror radii and spacing were varied until an eigenmode mode of each configuration was established. The beam diameter at the KTP crystal and at the YAG crystal were then recorded. These numbers could then be fed back into equation 22 of the previous section to determine the expected green output.

Computer Results

Two resonator designs have been identified that meet the needs of the laser. One design uses a plane parallel

YAG crystal 1cm in length. In this design, mirrors M1, and M2 in Figure 1 are both 15cm radius of curvature mirrors separated by ~ 20 cm. The KTP crystal is located at a beam waist on the order of 0.005cm radius. The beam diameter at the YAG crystal is on this order of 0.1cm and mirror M3 is a 50cm radius of curvature mirror. In this design, only one beam waist occurs inside the resonator, namely the one at the KTP crystal. This design should be fairly easy to align but will suffer from weak mode control.

A second design has been identified that has two beam waists. In this design, M1 is a 15cm radius of curvature mirror and M2 is a 25cm radius of curvature mirror. A beam waist exists between these mirrors on the order of 0.005cm radius. The beam is essentially collimated in the region between mirror M2 and the YAG crystal. The crystal is cut with a convex surface of radius 25cm. Mirror M3 is a 15cm radius of curvature mirror. In the space between M3 and the YAG crystal, a beam waist will also exist. This resonator will undoubtedly be very difficult to align. The existence of the second beam waist will provide a location for an aperture that can serve as a mode control aperture. The beam diameter at the YAG crystal in this resonator is on the order of 0.16mm, somewhat larger than desired.

A computer program was written to analyze equation 22 using the beam diameters at the KTP crystal and the YAG crystal determined from the previous code. The same code was also used to predict the output power that would have been observed by Durkin and Post. This serves as verification of the code. Over all, there is fair agreement between the code and the results reported by Durkin and Post. Computed and reported values are within 50% which, considering the number of parameters that are simply not known, is acceptable.

Consider first a case where the beam spot size (radius) at the KTP crystal is 0.005cm. At the YAG crystal, the pump and laser beams are both assumed equal and have spot size 0.062cm. As will be shown shortly, the values can be achieved with a resonator having a single beam waist at the KTP crystal. Figure 3 shows the predicted output power for this case. Pump input has been varied up to 15 watts (16 watts are available). 10% green coupling loss is assumed. The resonator loss is assumed to be 4% and the YAG crystal losses 1%. These are reasonable for a well designed set of mirrors. The code predicts in excess of 2 watts will be obtained using these components.

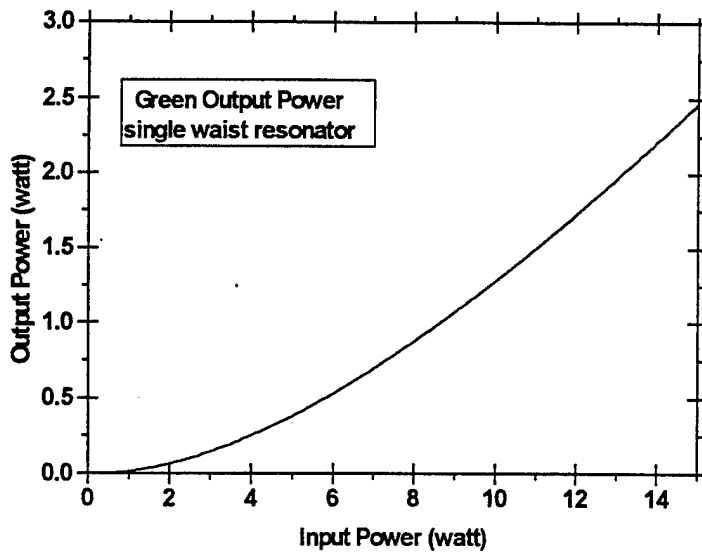


Figure 3

Predicted output using single waist resonator shown in Figure four.

be against oscillation of higher order modes. The code used to calculate the resonator performance assumed a lowest

The beam radius calculated as a function of position inside a resonator that achieves these parameters is shown in Figure 4. The beam in this case exhibits only one waist where the KTP crystal is located. The locations of the other components shown in figure 1 are also indicated in the figure. It is not clear how stable this resonator will

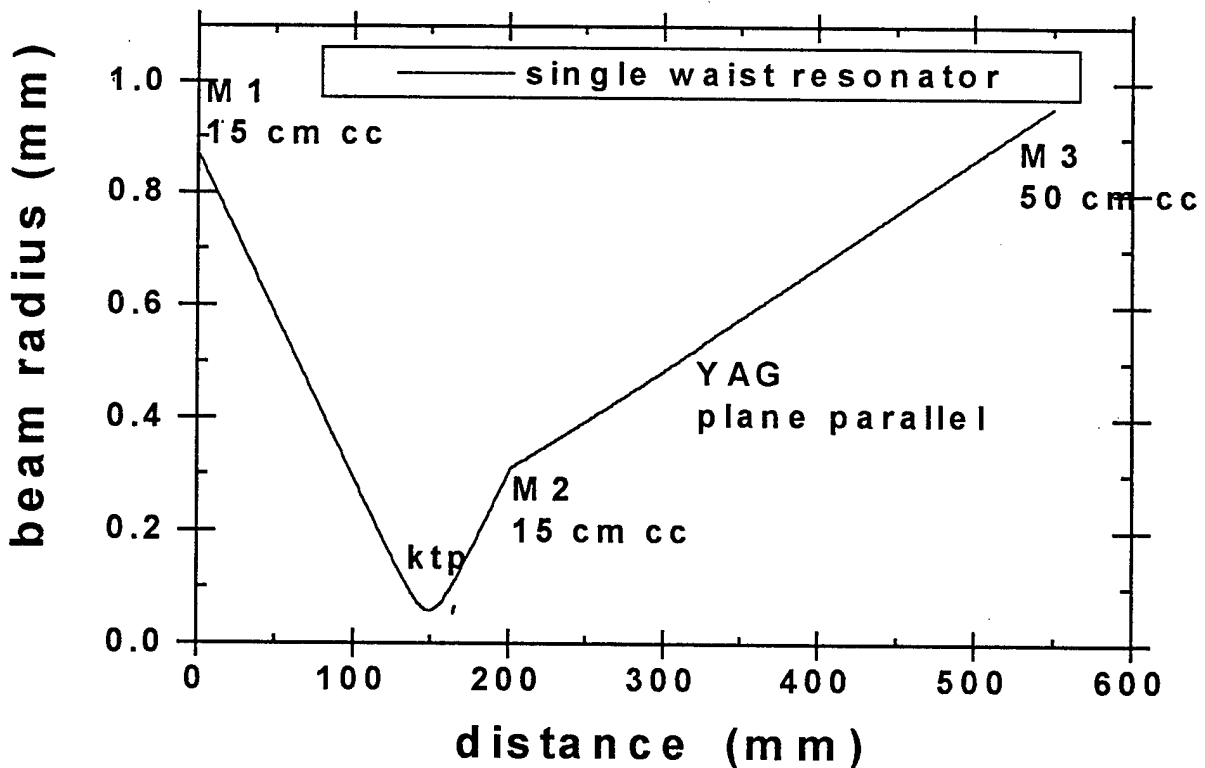


Figure 4

Beam radius as a function of position using a single waist resonator.

order mode (gaussian beam). The code is perfectly general and can be used to calculate any other modal distribution with only simple modifications. Such calculations have not at this time been carried out.

In intracavity doubling, thermal lensing at the YAG crystal and heating of the KTP crystal can cause the beam to find an alternate path inside the resonator resulting in reduced second harmonic output. The beam may also oscillate in higher order modes that are not efficiently doubled. To avoid some of the problems above, and provide good rejection against high order modes, a resonator with two beam waists can be used. At one beam waist the KTP crystal is located. The second beam waist is fitted with an aperture. The size of the aperture is chosen to allow only the lowest gaussian mode to pass with no losses, in this manner, high order modes are rejected.

An example of a two waist resonator is shown in Figure 5. In this case the spot size at the KTP crystal is essentially as before. The spot size at the YAG crystal is about 3% smaller and not surprisingly, some what higher output is achieved as shown in Figure 6.

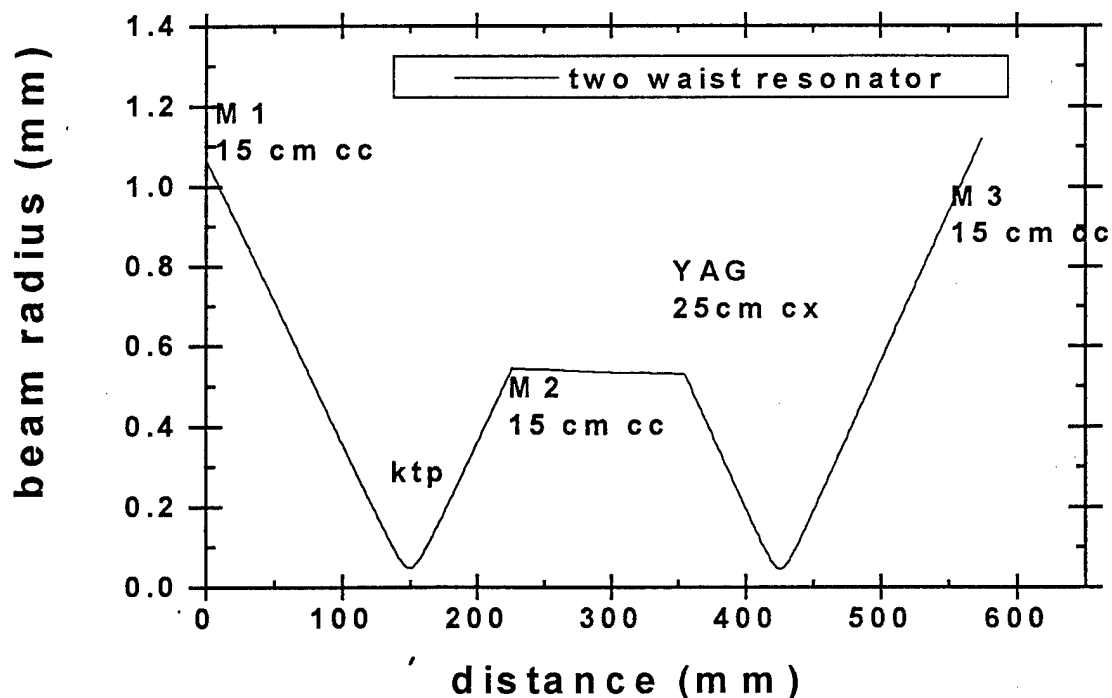


Figure 5
Beam radius as a function of position
using a symmetric waist resonator.

Laser Experiments

A breadboard prototype of the laser described by Durkin and Post was assembled

on an optical table. The laser used a fiber coupled diode array pump source. Figure 7 shows the output of the diode array plotted as a function of input current. Although the diode manufacturer claims up to 12 watts output at 808nm, testing has failed to achieve more than ~ 9.5 watts at 802nm. Also found to be out of spec was the diode laser array output wavelength. Again the manufacturer claimed the wavelength to be 808nm at room temperature, but testing has shown otherwise. Figure 8 shows the wavelength of the diode array recorded as a function of temperature at 24 amps input current. Typical output is on the order of 8.5 watts with the diode laser heated to achieve > 805nm.

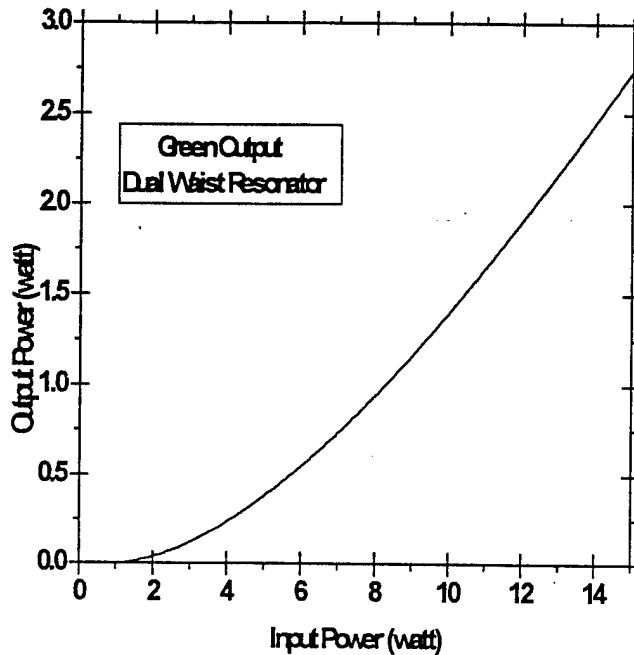


Figure 6
Predicted output using the symmetrical waist resonator shown on Figure 5.

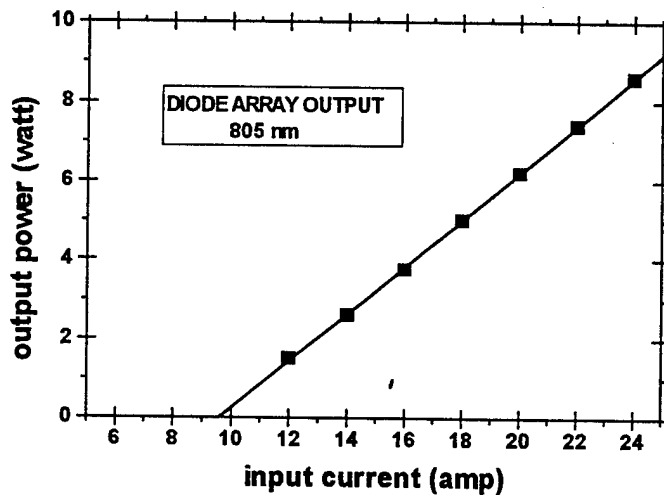


Figure 7
Laser Diode array output.

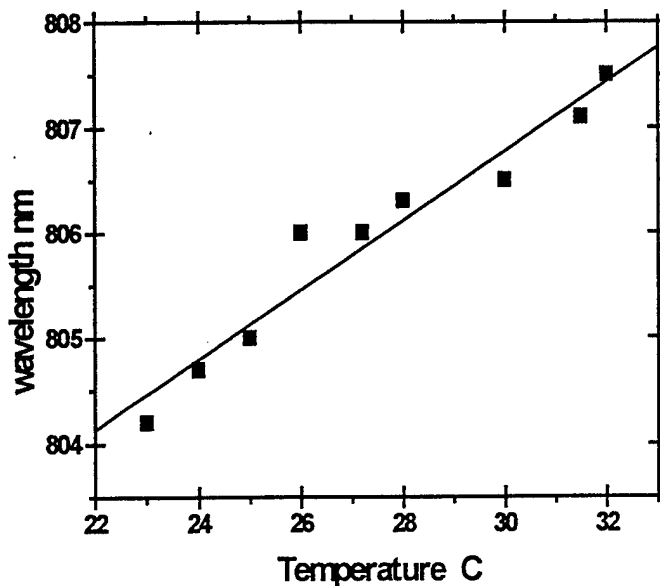


Figure 8
Temperature dependence of
diode array output.

for the round trip losses. For future design work, the value 3% has been adopted.

With a KTP crystal the beam waist location, green

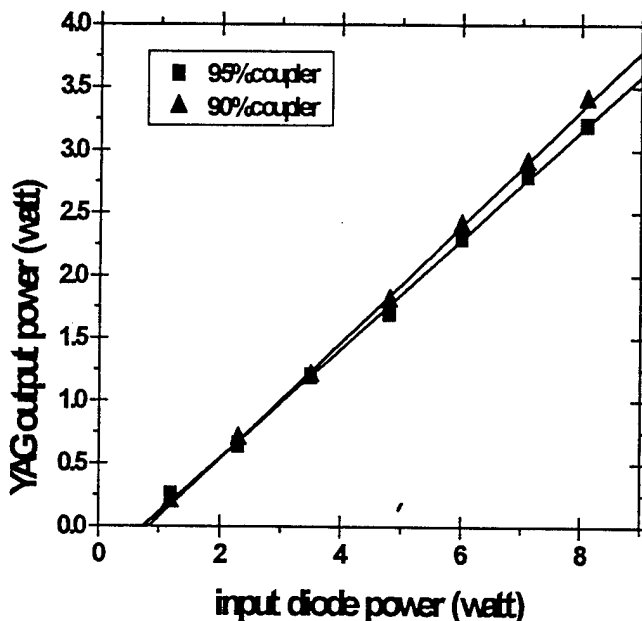


Figure 9
YAG laser output

The breadboard laser has been investigated as a common Nd:YAG laser and in excess of 45% efficiency demonstrated. Typical data are presented in Figure 9 using both a 95% reflective and a 90% reflective output coupler. Slope efficiency and threshold have been measured for this laser and estimates of the losses made from this data. The estimates range from ~ 1% to ~ 4%

output was readily obtained. It is convenient to run the laser with a 1.06um output coupler and a KTP crystal. In this manner the circulating power inside the resonator at 1.06um can be determined from the infrared output. Green output can also be measured and compared with model predictions. The results are given in Table I below. Here, green output is shown for two values of the circulating power.

The model predictions are also shown.

Input	8.4 w
Power:	
losses:	3%
Beam	@ KTP:
Radius:	0.11mm
	@ YAG:
	0.25mm

OUTPUT COUPLER (REFLECTIVITY)	CIRCULATING POWER (w)		GREEN OUTPUT (mw)	
	measured	calculated	measured	calculated
.9	51	63.3	85	134
.944	101	94.3	300	298
1.0	-	168.4	1000	951

Table I
Summary of Green Laser Performance

One aspect of the laser operations that was not expected was the great sensitivity of the laser to small alignment variations and difficulty in achieving high output reliability. Discussion with P. Durkin led to the introduction of a quarter wave plate into the resonator. The laser became far more stable and could be aligned easily to achieve the highest output. Best results to date have demonstrated 1.5 w of green output with ~ 10.5 w of pump diode power in reasonable agreement with expected performance.

II.2 Objective 2) In-vitro and In-vivo tests.

As already indicated, a series of experimennts, both in-vitro and in-vivo were planned to establish the safety of the frequency doubled YAG laser. Direct comparison with tissue exposures using an argon ion laser at identical parameters were planned. In-vitro experiments provide information on the acute response of the tissue to irradiation. In-vivo exposures permit investigation in a model where healing response can also be evaluated. Although not all the experiments planned were completed, all data indicate tissue response to the frequency doubled YAG laser to be largely the same as the response to the argon ion laser. This result is largely as expected and supports extension of the program into clinical studies in Phase II.

In-Vitro Testing

The purpose of the in-vitro testing is compare the acute response of ocular tissue to the frequency doubled YAG laser. Autopsy animal eyes (pig) were mounted in a container designed for this purpose,¹⁶ For laser trabeculoplasty, the pigmented trabecular meshwork was mounted in the eye container. Using this model, typical settings for the laser were 500-700mW, 0.1 s, and 100 um spot size. The typical response is small bubble formation and mild blanching. Iris sections were also mounted in the eye containers to test iridoplasty and iridectomy. Iridoplasty was performed with laser settings of 100um spot size, 500-700 mW, 0.1s. Exposed tissues were examined histologically. The area of thermal damage was assessed with a micrometer.

In-Vivo Testing

Use of the frequency doubled YAG laser was tested in-vivo in rabbits. New Zealand white albino rabbits weighing between 3.5 to 4.5 kg were used in this study. All aspects of this study were carried out in accordance with the Association for Research in Vision and Ophthalmology (ARVO) resolution on the use of animals in research. All experiment protocols were reviewed by the animal use committee at the Massachusetts Eye and Ear Infirmary prior to the initiation of any work. Anesthesia was achieved with intramuscular injections of ketamine hydrochloride (35 mg/kg) and xylazine hydrochloride (5 mg/kg) in the hind leg area. After the procedure, the eyes were treated with iopidine and prednisone acetate eyedrops.

To study the tissue effects of the laser, the eyes were enucleated after pentobarbitol (25 mg/kg) was administered intravenously. Histological studies were performed on eyes harvested both immediately after the laser procedure and 6 weeks after the laser procedure. The latter to assess the wound healing response. After enucleation, the rabbits were sacrificed with an overdose of pentobarbitol.

Laser Iridotomy

Immediately upon delivery of the laser, iridotomies were performed on freshly harvested pig eyes. Treatment parameters were 500 mw laser power, 0.1 sec exposures, 100 um laser spot. Direct comparison with an Argon ion laser operating at the same power was performed. One surprising result has been the effectiveness of the frequency doubled

YAG laser at penetrating the tissue. Although quantitative data are not sufficient to unequivocally support the conclusion, it appears the Nd:YAG is more effective at removing the tissue. In thin sections of the iris a single pulse from the YAG laser could drill clear through the iris. The Argon ion laser in the same region required up to 5 pulses to drill clear through the iris. This result was totally unexpected. More experiments are clearly needed to verify this result.

As outlined on the animal protocol, the animals were anesthetized by intra-muscular injection of ketamine hydrochloride (50mg/kg) and Xylazine (2mg/kg) and the eyes topically anesthetized with proparacaine hydrochloride. The animals were sacrificed by IV injection of pentobarbital sodium while still anesthetized. Samples were harvested for light microscopy, histology, and scanning electron microscopy. Figure 10 shows a scanning electron micrograph of a typical rabbit's eye treated with both the diode pumped frequency doubled YAG laser and the argon ion laser. Patent

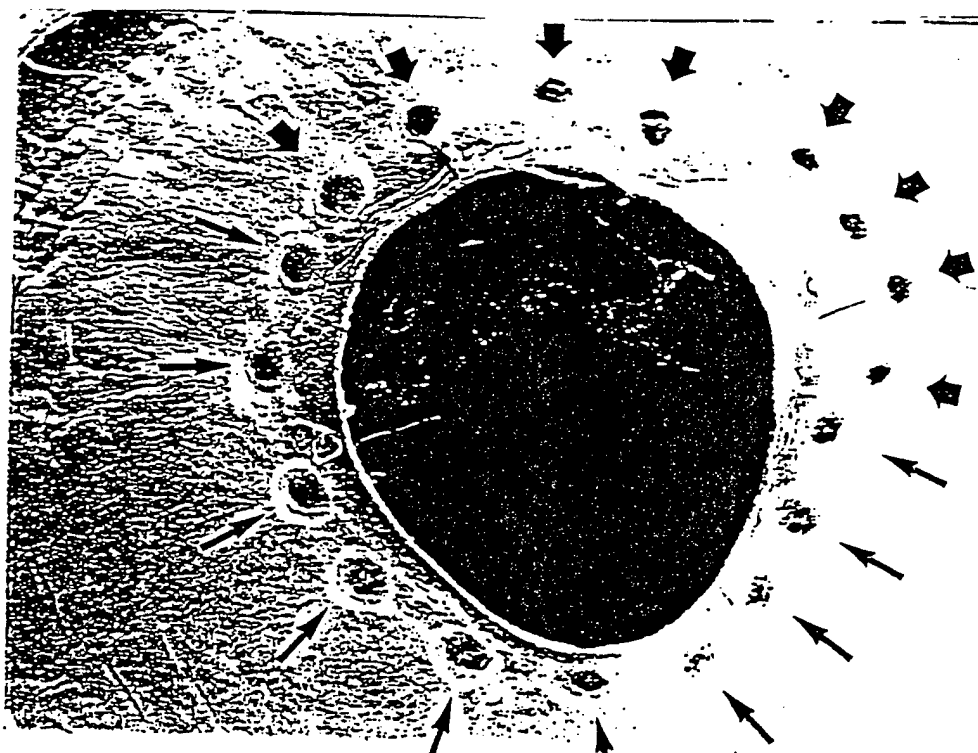


FIGURE 10

Scanning electron micrograph showing a planar view of the iris. Patent iridectomies were created with argon laser (arrow) and DPFDNd:YAG laser (arrow head) (magnification X32).

iridotomies were created with both lasers. Both lasers were calibrated to 0.5 w at the treatment site. Laser spot size was in both cases 0.1 mm and pulse duration was 0.1 sec.

Samples from similarly treated eyes were prepared and examined by thin section light microscopy, scanning electron microscopy and by gross histology.

For thin-section light microscopy enucleated eyes were fixed in 10% formalin, dissected, and dehydrated in ethanol up to 95%. The specimens were then embedded in Historesin and sectioned at 3 μ m with glass knife using Histo-range (LKB). Serial sections throughout the area of iridectomy were performed and the sections were stained with hematoxylin and eosin. Figure 11 shows typical cross section views of two iridotomies. The one on the left (A) was produced using the argon ion laser while the one on the right was produced using the diode pumped laser (D). The zone of thermal damage in each case is indicated by the arrows and is largely the same in both cases. Twenty sections from eight iridectomies in each group were examined

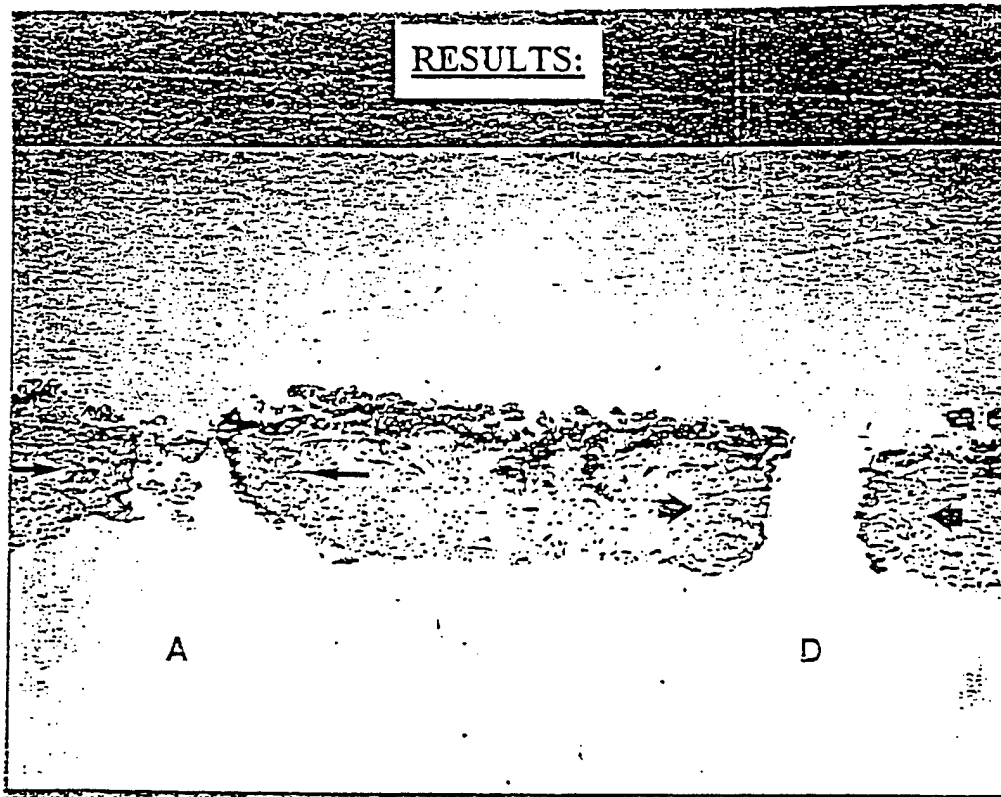


FIGURE 11

Light micrograph showing cross section view of two iridectomies produced by the argon laser (A) on the left and the DPFDNd:YAG laser (D) on the right. Note thermal damage zone in the iris by the argon laser (arrow) and by the DPFDNd:YAG laser (arrow head) (Hematoxylin and eosin, magnification X35).

for thermal damage of the collateral tissues using a calibrated micrometer reticle. The statistical significant differences between the groups were calculated using the

unpaired t-test. The mean zone of thermal damage were found to be $178 \pm 19 \mu\text{m}$ for iridotomies produced using the diode pumped laser, and $163 \pm 24 \mu\text{m}$ for those created using the argon ion laser.

For scanning electron microscopy, enucleated eyes were fixed in 1/2 strength Karnovsky's fixative, dissected and processed by dehydrating through a graded series of ethanol. The tissue was then dried in hexamethyldisilazane for one hour and air dried overnight. The dried pieces were mounted and then sputter coated with gold on Balzers SCD 040. The specimens were then examined and photographed on a scanning electron microscope (Amray AMR 1000A). Figure 12 shows a scanning electron micrograph of an iridectomy produced by an argon ion laser while a similar micrograph of an iridectomy produced using the diode pumped laser is shown in Figure 13. The zone of thermal damage is clearly identified in both cases.

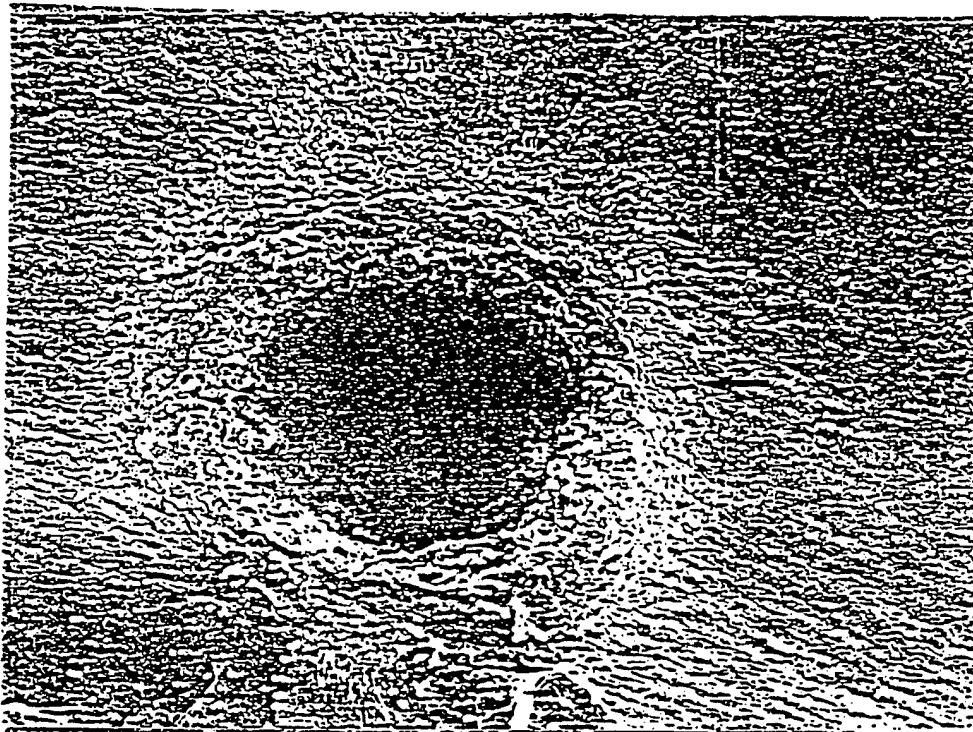


FIGURE 12
Scanning electron micrograph showing an iridectomy produced by the argon laser. Thermal damage zone in the iris indicated by arrow (magnification X300).

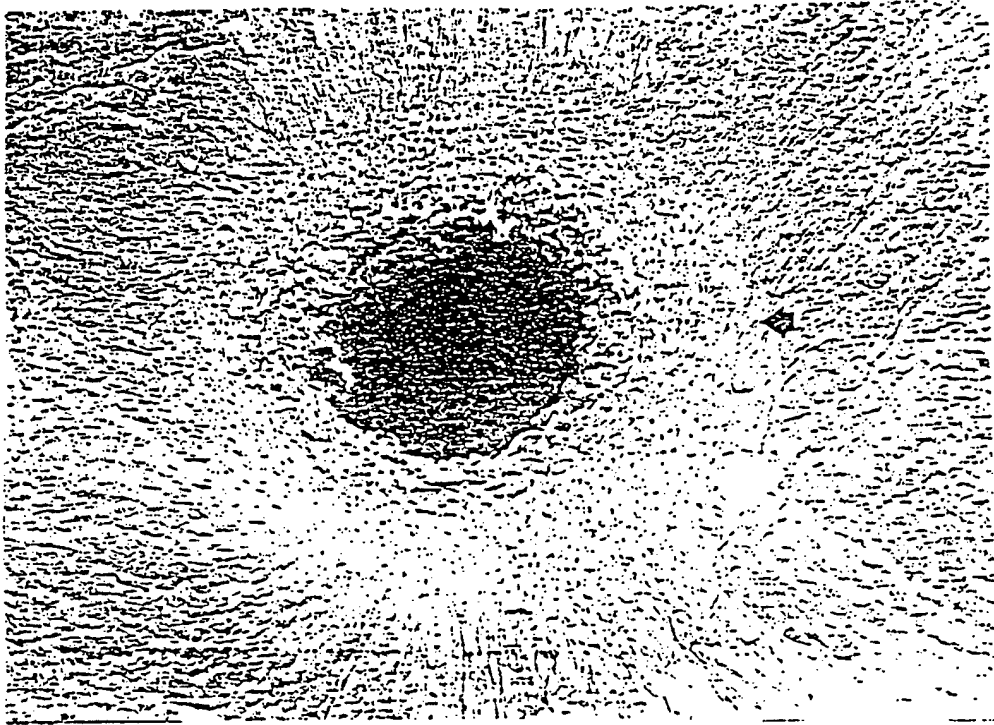


FIGURE 13

Scanning electron micrograph showing an iridectomy produced by the DPFdNd:YAG laser. Thermal damage zone in the iris indicated by arrow head (magnification X300).

Laser Iridotomy Results

The diode pumped frequency doubled YAG (DPFdNd:YAG) laser successfully created patent iridectomy in all animal eyes treated. Both the DPFdNd:YAG laser and the argon laser produced effects consistent with a thermal process. Gross and histologic evaluation showed similar thermal effects in iris tissues for both the DPFdNd:YAG and the argon laser. A concentric zone of coagulation necrosis was noted to occur and the lesions produced by both lasers produced a well-defined damage to the iris tissue. The mean zone of thermal damage was $178 \text{ um} \pm 19$ for the DPFdNd:YAG laser and $163 \text{ um} \pm 24$ for the argon laser (NS).

Laser Trabeculoplasty

The slit lamp delivery system used in the studies described here lacked an effective illumination source. For the iridotomy work described above, this is a tolerable shortcoming since the iris can be illuminated with an external source. For trabeculoplasty however this poses a major problem. Good illumination is needed at the trabecular meshwork in order to ensure a proper exposure. In the case of in vitro studies where the tissue samples are mounted with the trabecular meshwork exposed, the lack of an illumination source is again tolerable. In vivo studies were considered risky however. Rather than taking the risk of sacrificing animals for only marginal data, the in-vivo studies were dropped.

Freshly harvested pig eyes were dissected and tissue sections mounted in the container previously mentioned with sections of the trabecular meshwork exposed. A series of single pulse laser exposures were then performed with both the diode pumped laser and the argon ion laser. Laser parameters were 500-700mw, 0.1 sec exposure, and 100 μ m spot size. The acute response of the tissue was largely the same for both lasers. In each case, tissue blanching and bubble formation were observed. Light microscopy of typical exposures revealed similar tissue response to both lasers.

Retinal Exposure

The wavelength of the diode pumped frequency doubled YAG laser (532nm) is close to a peak in the absorption spectra of oxyhemoglobin. As a result, the laser radiation is strongly absorbed by vascular tissue. It is reasonable then to expect that this laser will make a good photocoagulation source. Retinal tissue is commonly treated by photocoagulation for conditions such as macular degeneration, the leading cause of blindness.

Although it was not originally proposed as part of the Phase I statement of work, retinal exposures were performed in-vitro in freshly harvested pig eyes. As before, the acute tissue response to the diode pumped laser was compared to the response to the argon ion laser. Single pulse laser exposures of 0.1 sec duration, 500 mw, and 100 μ m spot size were effected on dissected retinal sections of the eyes. Both the diode pumped laser and the argon ion laser were used. Similar tissue response were observed in both cases. While this result is encouraging, it is imperative that in-vivo tests be carried out since it is in oxyhemoglobin rich tissue that the real response of the tissue to each of the lasers will be evident.

Laser Suturelysis

Laser suturelysis is a common adjunct procedure to sclerostomy. It is common during a sclerostomy procedure to apply a suture at the sclerostomy site. The conjunctiva is then replaced over the sclerostomy site and the suture is cut by exposure to pulses from an argon ion laser. To test the effectiveness of the diode pumped laser for use in suturelysis, a white, #5 suture was placed under the conjunctiva above the sclera of a harvested eye. The suture was then exposed to repeated laser pulses of 0.1 sec duration, 500 mw and 0.1 mm spot size. The suture was cut with 11 pulses. There was no damage to the overlying conjunctiva and the suture was easily removed. This rather simple experiment is a more significant result than may at first be perceived. The portable nature of the diode pumped laser makes this laser easily available at any surgical site allowing the ophthalmologist to take advantage of this procedure without the need to move the patient to a site where an argon ion laser is available.

II.3. Objective 3) Investigation of Rectangular Core Fiber

Diode lasers are fabricated in the form of long narrow strip emitters. Typical high output power devices are capable of providing 10mw/ μ m of stripe. Thus to obtain output power on the order of ws, several hundred micrometer stripes are needed. If such a laser is coupled into an optical fiber of circular cross section, the initial brightness of the diode laser is greatly reduced. Roughly, the diode output power increases linearly with increasing stripe dimension, but the power per unit area from the fiber decreases as the square of the same dimension. The result is a net loss of system brightness.

If a rectangular core fiber is used, higher brightness is maintained limited only by the aspect ratio of the core. A number of preliminary experiments using rectangular core fibers were performed. Two fibers were investigated. These had core aspect ratios of 10:1 and 20:1. Both were of numerical aperture NA= 0.14.

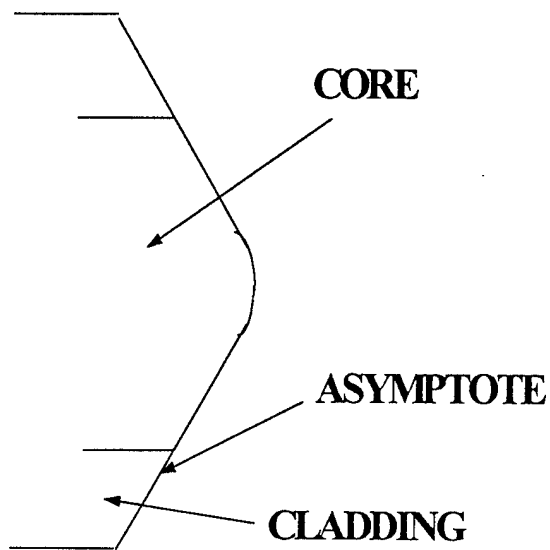


Figure 14
Cylindrical lens on fiber tip
approximating a hyperbolic shape.

The 10:1 fiber was drawn to a core dimension (long) of 200um. The fiber was then coupled to an 810nm diode laser of 80um stripe length. The numerical aperture of this is similar to that of typical laser emission along the direction of the laser stripe. Next a cylindrical lens was fabricated on the end of the fiber in the direction of the small

dimension of the rectangular core as shown in Figure 14. Ideally, the shape of the lens is given by a hyperbola. While it is difficult to achieve a hyperbola exactly, a hyperbolic shape can be approximated in two steps. First the fiber is fabricated into a sharp chisel point. Next the point is rounded to a radius on the order of 5um. The resulting curve will approximate the desired hyperbolic shape. Fabrication of lenses of this type was carried out by FFI staff on ordinary (circular core) multimode fiber prior to the STTR Phase I effort. Figure 15 shows a typical fiber section. The shape clearly approximates a hyperbola as described above.

Single fiber experiments using rectangular core fiber have been completed. Measured transmission of the radiation emitted from the diode bar is in the range of 48%-72%. As might be expected the transmission of the fiber was highly sensitive to angular misalignment of the fiber core with respect to the diode stripe. It was observed that a 5° misalignment error resulted in a 3dB output drop.

The 20:1 aspect ratio fiber was drawn to a core dimension (long) of 180um. The same 80um diode was coupled into this fiber. At best alignment, 48% of the diode output was transmitted through the fiber. Thus, the output from the

20:1 aspect ratio fiber exhibits approximately 16 times higher brightness than the same output power from a circular core fiber of diameter 180um and having the same numerical aperture as the rectangular fiber.

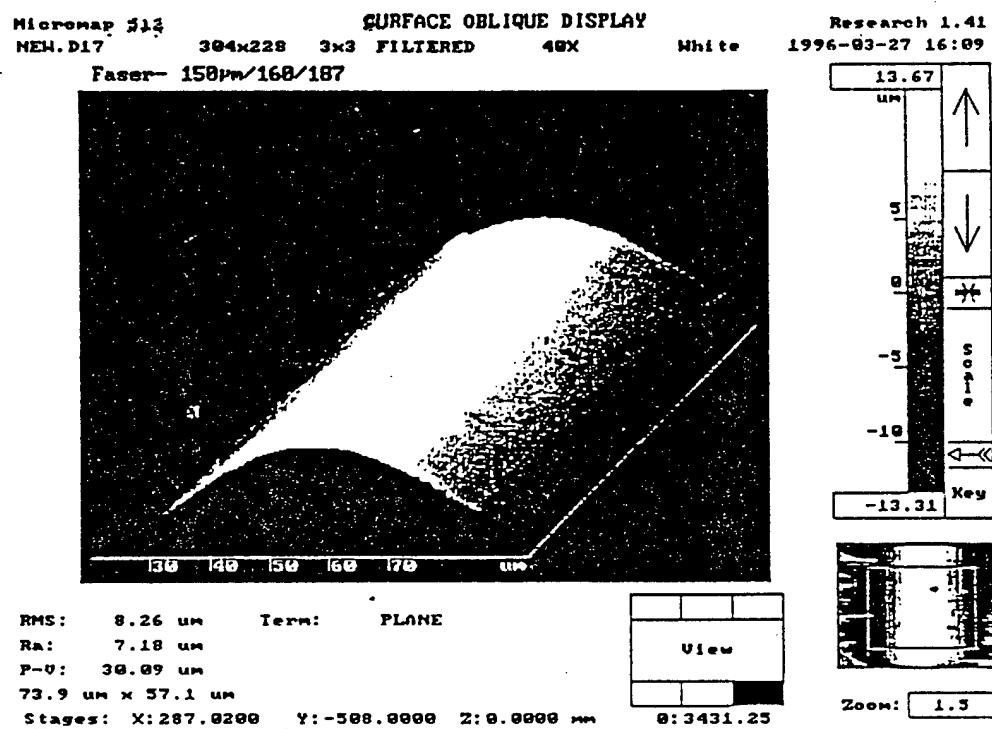


Figure 15
 Measured profile of cylindrical
 lens on fiber tip

The polarization maintaining properties of the fiber were also investigated. The output from diode lasers is typically linearly polarized with the electric field vector oriented along the plane of the stripe. In the absence of angular misalignment it is expected that reflections in the rectangular core fiber will not rotate the orientation of the electric field vector. As a result, the polarization of the radiation could remain linear.

Using a Glan Prism polarizer, the polarization of the diode source was analyzed and found to be linear with >10:1 contrast ratio of the two polarizations. The output from the rectangular core fiber was analyzed using the same prism and found to be largely linearly polarized with a contrast ratio of the two polarizations in excess of 8:1. At the time the experiments were carried out there was no way to orient the fiber accurately with respect to the diode stripe. One may expect the contrast ratio of the two polarizations to be at least 8:1 and probably higher.

III. Discussion

The Phase I objectives have been largely met. The laser design described by Durkin and Post has been found robust enough to be used in a medical environment. A prototype laser of this design was used in a series of in-vitro and in-vivo experiments. These experiments have established the safety of the laser for use in the management of glaucoma. Analysis of the laser design has been carried out and the use of rectangular core optical fibers to achieve a high brightness fiber coupled diode source has been investigated. The results in all cases has been consistent with initial expectations.

The most significant result of the work is verification of the assumption that the cw diode pumped frequency doubled YAG laser effects a tissue response nearly identical to that observed with an argon ion laser at identical power, spot size and pulse duration. In-vitro exposure of ocular tissue with both lasers showed an acute response consistent with a thermal process. A well defined concentric zone of coagulation necrosis was noted in the lesions produced with both lasers. The mean zone of thermal damage was statistically identical for exposures to the two lasers. All tests were performed using typical therapeutic laser parameters, suggesting the treatment settings for the frequency doubled YAG laser in clinical use will be essentially the same as those commonly used in argon ion laser procedures. This result will enhance the acceptability of the laser to the ophthalmic community.

The use of the frequency doubled YAG laser to treat retinal tissue and for laser suturelysis were also investigated. This was not part of the initial work plan, but extends the potential of the laser to encompass all ophthalmic applications currently performed with the argon ion laser. Continuation of both of these into clinical studies will also be carried out in Phase II.

The modeling of the laser design has provided a good understanding of the laser dynamics. In particular, the modeling was found to be in good agreement with observed results. It also suggested that a reliable 2.0 w green laser can be obtained with 15 w of input 808 nm pump power. A 1.5 w green laser is currently being commercialized through licensing agreements with CeramOptec, a medical device manufacturer. The laser modeling effort will be continued into Phase II where scaling to higher output powers will be considered.

The efficiency of a laser pumped laser is often limited by the brightness of the pump source. If the pump source is delivered by means of an optical fiber, it is the optical

properties of the fiber (core size and numerical aperture) that limit the brightness of the source. In the case of diode laser sources, one has what is essentially a line source. Coupling into a circular core fiber necessarily reduces the source brightness.

The use of a rectangular core geometry permits the designer to maintain a larger overall brightness. Two fibers were fabricated and tested during Phase I. Cylindrical lenses were successfully polished onto the fiber tips. The lenses were shaped to approximate a hyperbola. A hyperbolic shape is the ideal shape for coupling a large diverging source such as a laser diode. All experiments performed in Phase I involved the use of individual fibers. The extension to the use of high power laser diode arrays will be considered in Phase II.

In addition to the ability to provide a higher source brightness, rectangular core fibers will not randomize the state of polarization of the radiation from the diode laser. The experiments carried out during Phase I showed at least an 8:1 contrast ratio of the two linear polarizations at the distal end of the fiber. This result is probably not a limit, but the result of improper fiber alignment. The ability to maintain linear polarization opens the way for polarization combining of two fiber coupled diode arrays. It also can be exploited to pump polarization sensitive absorption bands in commonly used crystals such as Nd doped vanadates. Polarization combining of fiber coupled arrays is an objective of the Phase II program.

IV. Phase II Objectives.

The work performed under Phase I has largely met the objectives presented and serves as a good starting point for Phase II. There are four major objectives of the Phase II work. These are extensions of the work begun under Phase I and will lead to a number of commercial products. The objectives are

- a) Demonstration of the effectiveness of the diode pumped frequency doubled YAG laser for the management of both glaucoma and retinal abnormalities.
- b) Scale the existing 1.5 w output laser to output of the order of 3.0 w.
- c) Scale laser power beyond 3.0 w with a goal 15 w or greater.

d) Demonstrate very high brightness fiber coupling of diode bars to power densities in excess of 150 Kw/cm^2 through a single $100 \mu\text{m}$ core fiber of 0.2 numerical aperture.

The rationale, potential commercial applications, and probability of success of these objectives is now discussed.

Demonstrate the effectiveness of the Diode Pumped Frequency Doubled cw YAG Laser

During the Phase I effort, a low power diode pumped frequency doubled cw YAG laser was assembled and used to perform in-vitro and in-vivo iridectomies and trabeculoplasties. The results, presented at the Advanced Research in Vision and Ophthalmology (ARVO) meeting, showed the acute tissue response obtained using this laser to be essentially identical to that obtained using an argon ion laser. Based on that work and other considerations, FFI has applied for a license to use the Air Force technology and has begun commercializing the low power laser developed under Phase I.

Extension of this work to cover all areas of ophthalmology and demonstration of the laser in a clinical environment are clearly indicated for the Phase II effort. A key objective of the Phase II effort will be to demonstrate in a series of clinical trials, the efficacy of the laser in the treatment of glaucoma as well as retinal disease. With the addition of retinal indications the laser becomes a powerful tool to the ophthalmologist. Given the similarity between the acute tissue response to the frequency double YAG laser and that to the argon ion laser, one expects a high probability of success using the frequency doubled YAG laser. In the past others have used an arc lamp pumped frequency doubled YAG laser. There are reports of problems with stability and beam focusing using the arc lamp pumped laser that are not well documented but have resulted in some objections. The diode pumped laser used in Phase I was stable, the only instability being due to thermal changes. The output of the laser was typically coupled to a $50 \mu\text{m}$ core fiber whose numerical aperture was 0.1. Transmission of the laser radiation through the fiber was typically in the range of 80 to 85% of the input power. Any hot spots that may have exited in the beam are quickly homogenized after traversing one or two meters of the fiber. It is hard then to imagine what the earlier objections might have been and one expects a high probability of success in meeting this objective.

The Massachusetts Eye and Ear Infirmary will conduct both the glaucoma and the retinal clinical trials. Patients

will be recruited from the Boston area. Patient ethnic distribution will reflect the local distribution. Patients selected for treatment will be followed up for a period of at least six months. Analysis of the results will be compared to retrospective argon ion data.

Laser Development: Scale Laser Power to 3.0 w

The Phase I effort was carried out using a laser whose output was limited to about 1.5 w. While for most ophthalmic applications this is sufficient power, equipment such as slit lamps can introduce severe power penalties making the laser performance marginal in some cases. Scaling of the laser to higher output power would remove any limitations. The first milestone would be output in the range of 3.0 w. This target was chosen since it would bring the laser output in line with that of many argon ion lasers and output at this level has already been demonstrated by researchers at PL. It is interesting to note that the output of typical argon ion lasers is approximately equally divided between two wavelengths. These are 514 nm and 488nm. For many applications, particularly retinal applications the 488nm radiation is actually detrimental and must be filtered. For all those applications then, the 1.5 w laser is actually equivalent to a 3.0 w argon ion laser.

It is expected that the 3.0 w milestone will be achieved very early in the Phase II effort and that a 3.0 w laser will be commercialized beginning around the end of the first year of the Phase II effort. CeramOptec has committed to fund the commercialization of a 3.0 w laser.

Laser Development: Scale Laser Power Beyond 3.0 w

The list of applications of argon ion lasers in areas other than ophthalmology is extensive. It includes dermatology, otolaryngology, and general surgery. For many of the applications however higher powers are required. Argon ion lasers of output in excess of 15 w are very costly and require significant maintenance and service facilities. For this reason, the lasers have not gained much popularity among practitioners. Arc lamp excited frequency doubled YAG lasers repetitively Q-switched at high repetition rates provide output up to about 50 w. The lasers however are neither small nor inexpensive. A 40 w laser from LaserScope lists for \$140k. It is unlikely that this laser will drop significantly in price. Arc lamp excited lasers are a mature technology without the potential for a breakthrough that may drive the costs down. The cost of diode pumped lasers on the

other hand is largely dictated by the cost of the pump diodes, and these do have the potential for undergoing a significant reduction in cost. For this reason it makes sense to investigate the possibility of scaling even beyond what has been demonstrated thus far. Scaling of the laser beyond the 3 w output currently demonstrated is an objective of the Phase II effort. During the first year effort the problems to be overcome will be identified and resolved. Laser output in the range 10 to 15 w is an objective for the second year effort. Commercialization of these lasers will begin at the end of the Phase II effort.

High Brightness Fiber Coupled Diode Laser Bars

An area that has emerged as particularly valuable is the development of very high brightness fiber coupled diode bars. As part of the Phase I effort, the use of proprietary rectangular core fibers was investigated as a means of increasing the brightness of fiber coupled diode laser sources. It was thought at the beginning of the program that the brightness of fiber coupled pump diode laser sources would ultimately limit laser performance. This has not proven to be the case, limitations have resulted from other causes. Still, as the Phase I effort has progressed, it appears that the use of these proprietary fibers will result in high brightness devices. These would then find applications as laser pump sources for laser materials of low gain crosssection such as thulium. They would also find applications as pump sources for fiber lasers. Industrial applications that require very high brightness are also a potential area for their use. For these reasons continuation of this development is an objective of Phase II.

Using a proprietary technique ten circular core lensed fibers can be produced simultaneously and coupled to a ten emitter diode bar. Typical values of the transmitted power through a one meter length of fiber are in the range 65% to 75% of the power emitted by the bar. These fiber coupled diode bars are used as the pump source for the 1.5 w green laser currently undergoing commercialization. Extension of this fabrication technique to the use of the rectangular cross section fibers is an objective of the Phase II effort.

Rectangular core fibers can be used to fabricate fiber coupled illumination sources of very high brightness ($\text{w/cm}^2/\text{sr}$). At equal transmitted power and numerical aperture, the brightness at the distal end of a rectangular core fiber is much greater than that from a circular fiber of core diameter equal to the long rectangular dimension. The higher brightness can be exploited to couple multiple rectangular core fibers together. A procedure for coupling

multiple fibers together was discussed in the Phase I proposal.

A second significant benefit of rectangular core fibers relates to their ability to transmit linearly polarized radiation without significant depolarization. Tests have been carried out using diode lasers whose output is linearly polarized with the electric field vector transverse to the laser stripe. It is possible then to use the polarization maintaining property to combine the outputs of two linear fiber bundles and obtain at least a factor of 1.6 further increase in coupled power. Alternatively, the polarization maintaining properties may be exploited in laser pump sources for gain media whose pump absorption spectra depend strongly on the orientation of the electric field vector of the pump radiation.

V. Conclusions and Recommendations

The laser design described by Durkin and Post can be adapted to provide laser output suitable for therapeutic applications in ophthalmology. A prototype laser built at FFI was successfully used both in vitro and in vivo to perform surgical procedures commonly used in the management of glaucoma. The potential low cost and portable nature of the laser ensures the success of this laser commercially. In addition, access to laser treatment can be expanded to include those patients that have limited mobility or that are located in remote regions where the equivalent argon ion lasers may not be readily available.

All data demonstrated that tissue response to the frequency doubled YAG laser radiation is largely equivalent to the response of the tissue to the argon ion laser radiation at similar output power, pulse duration, and spot size. The Phase I work concentrated on procedures commonly used in the management of glaucoma. The great similarity between the tissue response to the frequency doubled YAG laser and to the argon ion laser supports expanding the indications for this laser to encompass all ophthalmic conditions commonly treated with the argon ion laser. Expansion of the work to include all ophthalmic indications currently addressed with the argon ion laser is recommended as part of the Phase II Work Statement.

While animal models can be used to establish the safety of a laser treatment, efficacy must be demonstrated in clinical studies. Based on the results of the Phase I study, clinical trials of procedures related to the management of glaucoma are indicated. The retinal data is at this time only preliminary, and clinical studies in this area will have to wait until the results of the in vitro and in vivo

studies proposed as part of the Phase II effort have been completed and analyzed.

One key element of the laser design described by Durkin and Post is the potential to scale the laser to higher output power. Higher output power will result in expanded application of the laser into other medical areas. These include dermatology, otolaryngology, and minimally invasive surgery. Scaling of the laser design to output power in excess of 10 watts is recommended for the Phase II effort.

V. Literature Cited

1. American Academy of Ophthalmology Quality Care Committee Glaucoma Panel: Primary Open Angle Glaucoma. San Francisco: American Academy of Ophthalmology, 1990.
2. U.S. Department of Health, Education and Welfare: Statistics on blindness in the model reporting area 1969-1970, DHEW Publication No NIH 73-427, Washington, DC, 1973, US Government Printing Office.
3. Martin MJ, Sommer A, Gold EB, Diamond EL: Race and primary open angle glaucoma. *AmJ Ophthalmol* 99: 383, 1985.
4. Wilensky JT, Gandhi N, Pan T: Racial influence in open angle glaucoma. *Ann Ophthalmol* 10: 1398, 1978.
5. Wilson MR, Hertzmark E, Waler AM, Childs-Shaw K, Epstein DL: a case-control study of risk factors in open-angle glaucoma. *Arch Ophthalmol* 105: 1066, 1987.
6. Mason RP, Kosoko O, Wilson MR, et al: National survey of the prevalence and risk factors of glaucoma in St. Lucia, West Indies, I: prevalence findings. *Ophthalmology* 96: 1363, 1989.
7. Wallace J, Lovell HG: Glaucoma and intraocular pressure in Jamaica. *Am J ophthalmol* 67: 93, 1969.
8. Frydman JE, Clower JW, Fulghum JE, Hester Mw: Glaucoma detection in Florida. *JAMA* 198: 1237, 1966.
9. Coulehan JL, Helzlsouer KJ, Rogers KD, Brown SI: Racial differences in intraocular tension and glaucoma surgery. *Am J Epidemiol* 111: 759, 1980.
10. Tielsch JM, Sommer A, Katz J, Royal RM, Quigley HA, Javitt S: Racial variations in the prevalence of primary open-angle glaucoma. The Baltimore Eye Survey. *JAMA* 266:369, 1991.
11. Belcher DC III, Greff LJ: Laser therapy of angle-closure glaucoma. In, Albert DM, Jakobiec FA, eds: *Principles and Practice of Ophthalmology*. Philadelphia, WB Saunders, 1994, pp 1597-1609.
12. Richter CU: Laser Therapy of open-angle glaucoma. In, Albert DM, Jakobiec FA, eds: *Principles and Practice of Ophthalmology*. Philadelphia WB Saunders, 1994, pp 1588-1597.
13. Smith SD, Netland PA: The role of laser trabeculoplasty as primary therapy for open-angle glaucoma. *Int Ophthalmol Clinics* 34: 149-161, 1994.
14. Shingleton BJ, Richter CU, Dharma SK et al: Long-term efficacy of argon laser trabeculoplasty: a 10 year follow up. *Ophthalmology* 1993: 100: 1324-9.
15. Chi TSK, Berrios RR, Netland PA: holmium laser sclerostomy via corneal approach with transconjunctival mitomycin C in rabbits. *Ophthalmic Surg*, in press, 1995.
16. Minckler, Gaasterland, and Erickson: improved, reusable, autopsy eye model container for laser trabeculoplasty and iridectomy. *Am J Ophthalmol* 113: 341, 1992.
17. Karp CL, Higginbotham EJ, Edward DP, Musch DC. Diode laser surgery: ab interno and ab externo versus conventional surgery in rabbits. *Ophthalmology* 1993:100 1567-1573.

18. Hoskins HD Jr, Iwach AG, Drake MV, et al.
Subconjunctival THC:YAG laser limbal sclerostomy ab externo in the rabbit. Ophthalmic Surg. 1990;21:589-592.
19. Iwach AB, Hoskins Jr HD, Drake MV, Dickens CJ.
Subconjunctival THC:YAG ["Holmium"] laser thermal sclerostomy ab externo: a one-year report. Ophthalmology. 1993;100:356-366.
20. Schuman JS, Stinson WG, Hutchinson BT, Bellows AR, Puliafito CA, Lytle R. Holmium laser sclerectomy: success and complications. Ophthalmology. 1993;100:1060-1065.
21. Iwach AG, Hoskins Jr HD, Drake MV, Dickens CJ.
Update of the subconjunctival THC:YAG [Holmium] laser sclerostomy ab externo clinical trial: 30-month report. Ophthalmic Surg. 1994;25:13-2.
22. Shields SR, Netland PA, Kalina PH, Cotran PR. Wrbium laser sclerostomy via transcorneal approach in rabbits. Invest Iphthalmol Vis Sci 1993;34(suppl);1071.
23. Schuman JS, . Namazi N, Wang N, Woods W, Shingleton BJ, Bellows Ar. Transconjunctival Mitomycin-C with Holmium laser sclerectomy in rabbits and humans. Invest Ophthalmol Vis Sci 1993;34(suppl):1071
24. March WF, Gherezghiher T, Koss MC, Nordquist RE.
Experimental YAG laser Sclerostomy. Arch Ophthalmol. 1984;102:1824-1836.
25. Latina M, Goode S, de Kater Aw, Long FH, Deutsch TF, Epstein DL. Experimental ab interno sclerostomies using a pulsed-dye laser. Laser Surg Med. 1988;8:233-240.
26. Feldman RM, Oram O, Gross Rl, Orengo-Nania S, Font RL. Histopathologic characteristics of failed holmium laser sclerostomy. Am J Ophthalmol 1993;116:766-767.
27. Miller MH, Grierson I, Unger Wi, Hitchings RA. Wound healing in an animal model of glaucoma fistulizing surgery in the rabbit. Ophthalmic Surg. 1989;20:350-357.
28. P.S. Durkin and S.G. Post "Compact, Continuous Wave, 1.2 w, Diode-Pumped Solid-State Laser" OSA proceedings on advanced solidstate lasers (1994).
29. W.A. Clarkson, I.I. Martin, and D.C. Hanna "High Power Single-Frequency Operation and Efficient Intracavity Frequency Doubling of a Nd:YAG, End Pumped By a 20 w Diode Bar" CLEO '95, Baltimore May 1995.

DISTRIBUTION LIST

AUL/LSE Bldg 1405 - 600 Chennault Circle Maxwell AFB, AL 36112-6424	1 cy
DTIC/OCP 8725 John J. Kingman Rd, Suite 0944 Ft Belvoir, VA 22060-6218	2 cys
AFSAA/SAI 1580 Air Force Pentagon Washington, DC 20330-1580	1 cy
PL/SUL Kirtland AFB, NM 87117-5776	2 cys
PL/HO Kirtland AFB, NM 87117-5776	1 cy
Official Record Copy PL/LIDA/Peter S. Durkin	4 cys